ELT-HIRES the high resolution instrument for the ELT: optical design and instrument architecture

Oliva, E., Tozzi, A., Ferruzzi, D., Riva, M., Genoni, M., et al.

E. Oliva, A. Tozzi, D. Ferruzzi, M. Riva, M. Genoni, A. Marconi, R. Maiolino, L. Origlia, "ELT-HIRES the high resolution instrument for the ELT: optical design and instrument architecture," Proc. SPIE 10702, Ground-based and Airborne Instrumentation for Astronomy VII, 107028O (8 July 2018); doi: 10.1117/12.2309923

SPIE.

Event: SPIE Astronomical Telescopes + Instrumentation, 2018, Austin, Texas, United States

ELT-HIRES the high resolution instrument for the ELT: optical design and instrument architecture

E. Oliva*[a], A. Tozzi[a] , D. Ferruzzi[a], M. Riva[b], M. Genoni[b], A. Marconi[a,c], R. Maiolino[d], L. Origlia[e]

[a] INAF-Arcetri Observatory, largo E. Fermi 5, I-50125 Firenze, Italy;
[b] INAF- Osservatorio Astronomico di Brera Via Bianchi 46, I-23807 Merate, Italy;
[c] Dip. Fisica e Astronomia, Univ. di Firenze, via G. Sansone 1, I-50019, Sesto Fiorentino (FI), Italy;
[d] Cavendish Laboratory University of Cambridge, 19 JJ Thomson Ave, Cambridge CB3 0HE, UK;
[e] INAF-Osservatorio Astronomico di Bologna, via P. Gobetti 93/3, I-40129, Bologna, Italy

ABSTRACT

The first generation of ELT instruments will include an optical-infrared High Resolution Spectrograph, conventionally indicated as ELT-HIRES. This paper describes the optical design and overall architecture of the instrument whose main capabilities can be summarized as follows.

- Fibers fed specrographs with resolving power R=100,000 (HR-modes), R=150,000 (UHR-modes) and R=20,000 (MR-modes).
- Simultaneous wavelength coverage from 400 nm to 1800 nm; extendable to 300-2400 nm.
- Spectrometers with fixed configurations and without moving optical parts.
- Maximum size of entrance apertures ideal for seeing limited observations.
- Many observing modes, including seeing-limited single-object spectroscopy, multi-objects medium resolution spectroscopy and IFU observations with different spatial scales, down to the diffraction limit of the ELT telescope.
- Observing modes defined and selected in interfaces outside of the spectrographs.
- Modular design compatible with a minimal baseline that can be subsequently expanded and upgraded.

Keywords: Ground-based instruments, high resolution spectrographs, infrared spectrographs

1. INTRODUCTION

The European Extremely Large Telescope (ELT) will be the largest ground-based telescope at visible and infrared wavelengths. The flagship science cases supporting the successful ELT construction proposal were the detection of life signatures in Earth-like exo-planets and the direct detection of the cosmic expansion re-acceleration. It is no coincidence that both science cases require observations with a high-resolution spectrograph. When defining the ELT instrumentation, ESO commissioned two phase-A studies for high resolution spectrographs, namely CODEX[1] (covering the 370 nm – 710 nm wavelengths range) and SIMPLE[2] (covering the 840 nm – 2400 nm wavelengths range). The studies, completed in 2010, demonstrated the importance of optical and near-IR high-resolution spectroscopy at the ELT. ESO thus decided to include a High-REsolution Spectrograph (HIRES) in the ELT instrumentation roadmap. At the same time, the CODEX and SIMPLE consortia realized the great scientific importance of covering the optical and near-infrared spectral ranges simultaneously. This marked the birth of the consortium that responded to the ESO call for the phase-A study of HIRES in March 2016. The study was successfully concluded in April 2018. More details on the HIRES project, science and consortium can be found in the dedicated paper[3] presented at this conference.

*oliva@arcetri.astro.it; phone +39 0552752291

Ground-based and Airborne Instrumentation for Astronomy VII, edited by Christopher J. Evans, Luc Simard, Hideki Takami,
Proc. of SPIE Vol. 10702, 107028O · © 2018 SPIE · CCC code: 0277-786X/18/$18 · doi: 10.1117/12.2309923

2. OVERALL CONCEPT OF THE ELT-HIRES INSTRUMENT

The design consists of four spectrometer modules covering different wavelength bands; all fed by fibers (see Figure 1). Each spectrometer module is fed by a number of fiber bundles that correspond to the different observing modes. Inside the spectrometer each fiber bundle is connected to a linear array of micro-lenses that act as input slit. The input slits are mounted and fixed once forever.

The resolving power of a given bundle is determined by the core-size of the fibers. The baseline design (described in Section 4).includes 10 slits/bundles for R=100,000 (HR modes), 10 slits/bundles for R=150,000 (UHR modes) and 1 slit/bundle for R=20,000 (MR mode). Note that each spectrometer can host twice as many slits/bundles.

Different front-ends are used for seeing-limited HR/UHR observations, for SCAO-IFU observations and for MOS-MR observations. Each front-end includes dichroics that split the light to the spectrometer moduli. The active observing mode is selected using shutters in the front-ends and/or in the fiber-to-fiber interfaces.

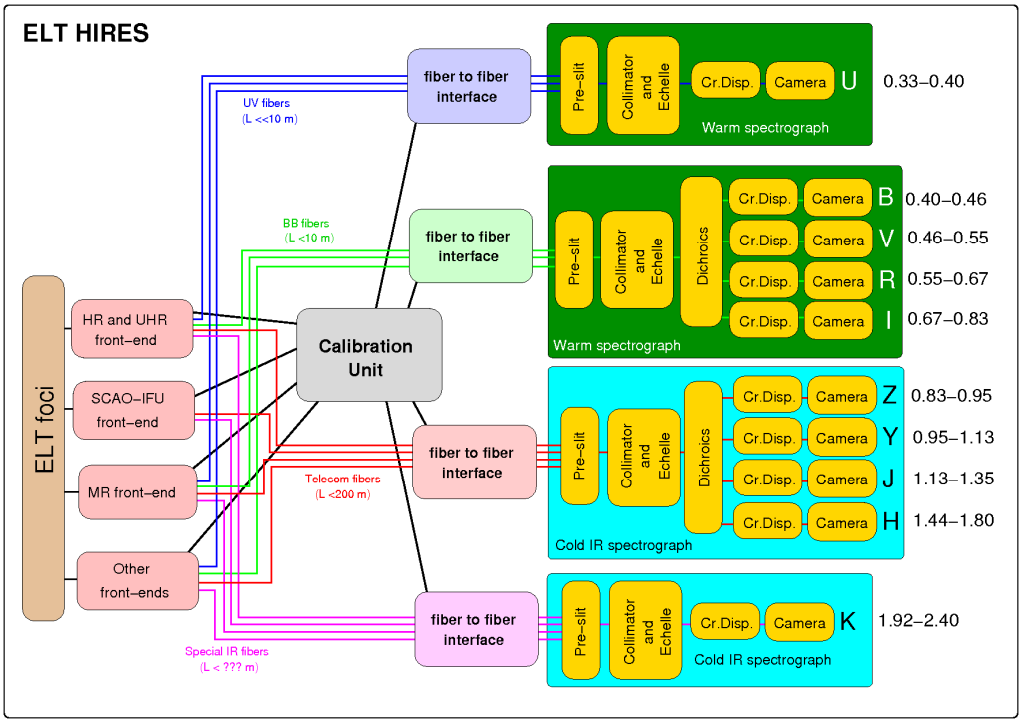

Figure 1 Schematic layout of the HIRES spectrometer; the numbers on the right-hand side are wavelengths in microns.

Outside the spectrometer the fiber bundles terminate into the fiber-to-fiber interfaces that include the opto-mechanical devices coupling the light into external fiber bundles that are connected to the telescope front-end or to the calibration unit. The topology of this coupling defines the details of each observing mode that can be set-up, maintained, modified or added without touching the spectrometer modules. The parameters of the baseline observing modes are summarized in Table 1. It includes

- 4 modes optimized for throughput; i.e. with as few as possible optical elements in the front-end[4] and in the fiber-to-fiber interfaces.
- 4 modes optimized for spectral accuracy; i.e. including - in the front-end and in the fiber-to-fiber inferfaces - opto-mechanical sub-systems that guarantee a uniform illumination of the fibers and of the spectrometer slit. These modes may result into some loss of efficiency, if necessary.
- 4 modes for spatial resolved spectroscopy; i.e. with the fiber-bundles organized for IFU observations in the dedicated front-end[5].

Other observing modes can be added later-on

Table 1 Main parameters of the baseline observing modes

Name	Type	Resolving power	# of sky apertures	Projected diameter of each fiber	# of fibers per aperture	Projected size of each aperture	Simultaneous calibration
B1	Throughput optimized	100,000	1	0.170”	64	Ø 1.36”	No
B2	Throughput optimized	100,000	2	0.170”	30	Ø 0.93”	No
B3	Throughput optimized	150,000	1	0.113”	96	Ø 1.11”	No
B4	Throughput optimized	150,000	2	0.113”	47	Ø 0.77”	No
B5	Accuracy optimized	100,000	1	0.170”	56	Ø 1.27”	Yes
B6	Accuracy optimized	100,000	2	0.170”	30	Ø 0.87”	Yes
B7	Accuracy optimized	150,000	1	0.133”	96	Ø 1.06”	Yes
B8	Accuracy optimized	150,000	2	0.133”	47	Ø 0.73”	Yes
A1a	Spatially resolved	100,000	1	0.010”	8 x 8	0.08” x 0.08”	No
A1b	Spatially resolved	100,000	1	0.100”	8 x 8	0.80” x 0.80”	No
A2a	Spatially resolved	150,000	1	0.010”	9 x 10	0.09” x 0.10”	No
A2b	Spatially resolved	150,000	1	0.100”	9 x 10	0.90” x 1.00”	No

3. THE SPECTROMETER MODULES

The functional scheme of a spectrometer module is depicted in Figure 2.

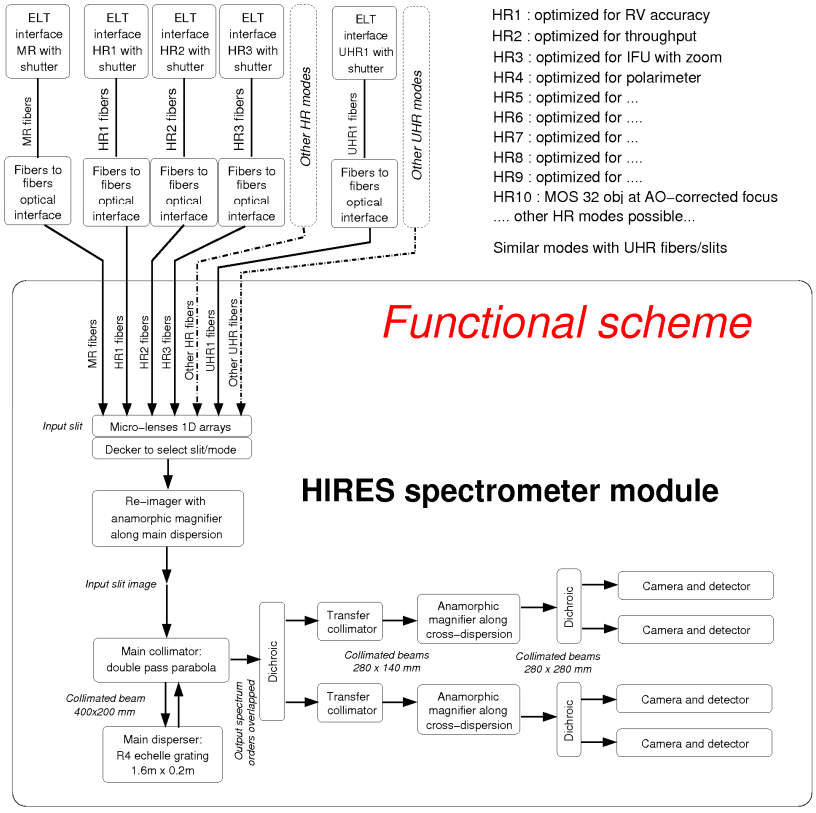

Figure 2 Functional scheme of a spectrometer module.

All the spectrometer modules are equipped with a number of adjacent, parallel slits all with a length equal to 11 arcsec (sky projected angle). The slit-resolution product of the spectrometer is RS=17,000. Therefore, the R=100,000 slits are made of 64 fibers with projected diameter 0.170 arcsec, while the R=150,000 slits are made by 96 fibers with projected diameter of 0.113 arcsec. The R=20,000 slits are made by 10 fibers with a projected diameter of 0.85 arcsec.

The main spectrometers (BVRI and ZYJH) include four separate arms covering wavelengths that are adjusted to maximize the wavelength coverage and overlap with the regions of good telluric transmission (see Figure 3). The U and K modules are added to push the coverage toward the UV and infrared domains. The K module requires different type of fibers (see Figure 4).

Indeed, the spectral range covered by the Z arm (830-950 nm) would be much more efficiently covered using a deep-depleted CCD detector in a non-cryogenic module. The Z-arm is included in the IR cryogenic module solely to push to the wavelength coverage of the BVRI module to the shorter possible wavelength. An alternative configuration with a three-arms IR module (YJH) covering the 950-1800 nm range would yield a more natural, efficient, and cost-effective solution that however limits the wavelength coverage achievable in the blue using just two moduli.

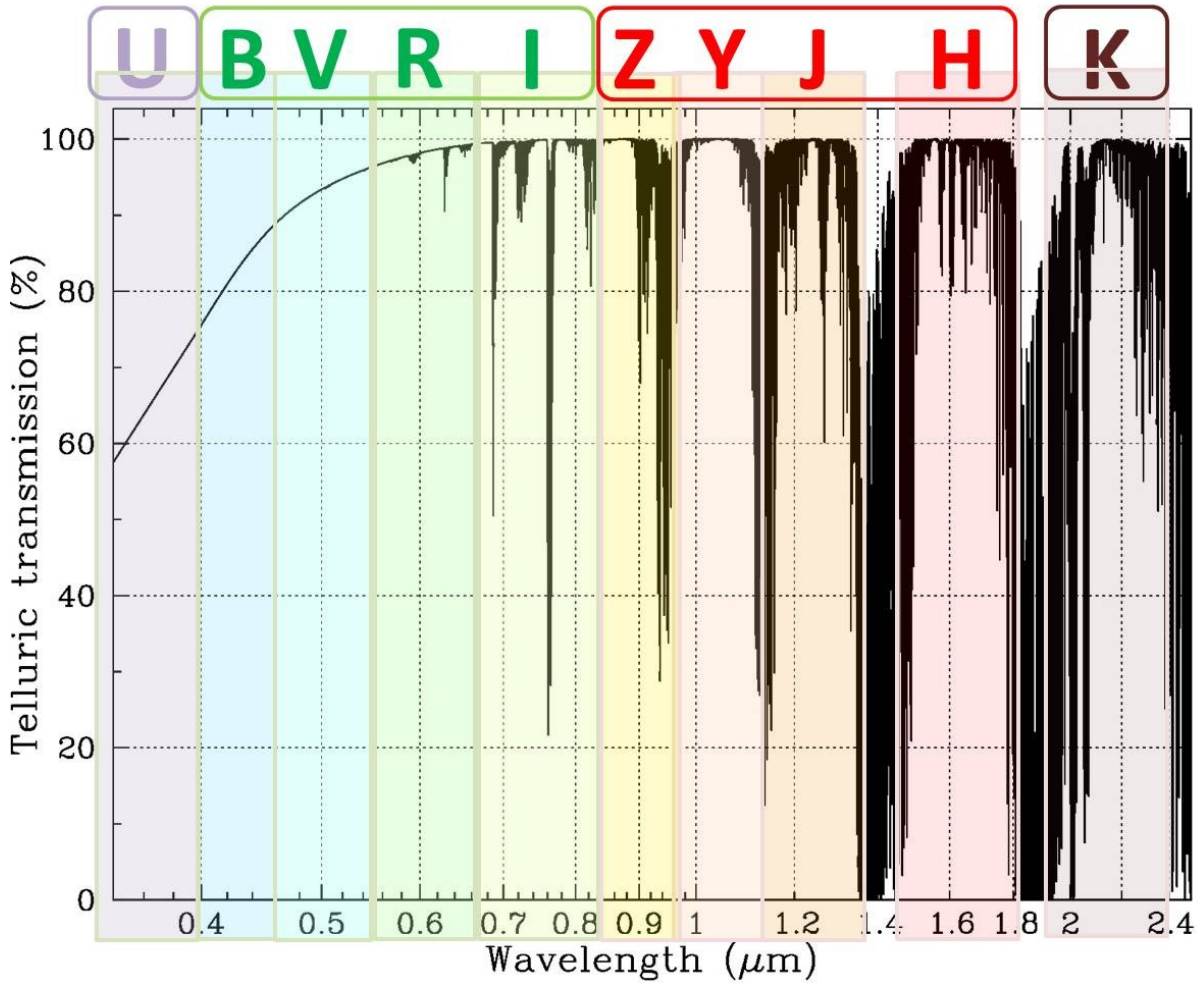

Figure 3 Telluric transmission (at air-mass=1) and wavelength coverage of the spectrometer modules

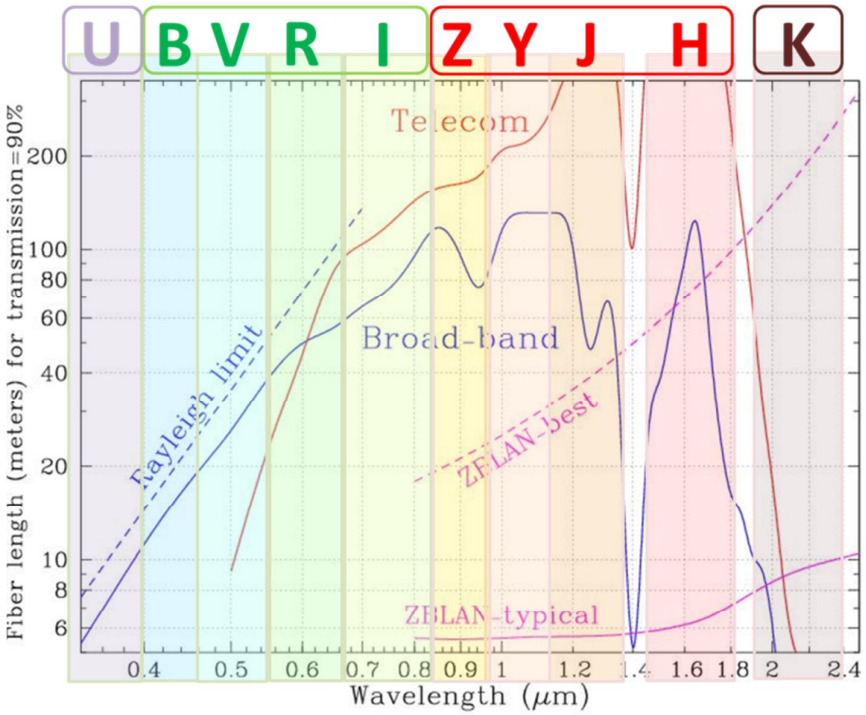

Figure 4 Transparency of different types of fibers and wavelength coverage of the spectrometer modules

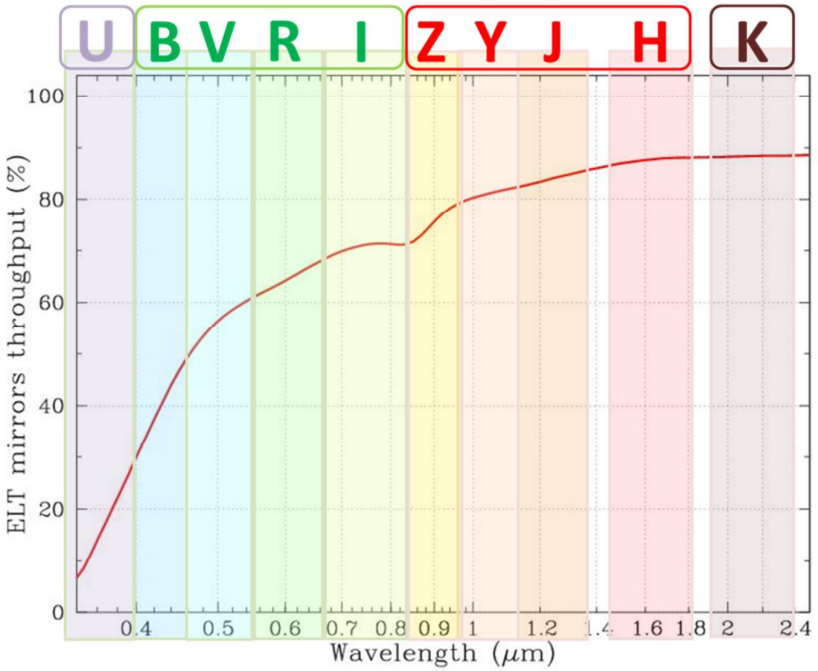

Figure 5 Throughput of the ELT mirrors and wavelength coverage of the spectrometer module

The layout and rays-tracing of the ZYJH module are displayed in Figure 6 and Figure 7.
Following the light path one finds the following elements.

- The input slit, consisting of linear arrays of micro-lenses as described in the Section 7.
- A slit re-imager and anamorphic pupil expander that includes
  - A lens-doublet that collimates the light from the slit.
  - Two prisms that provide a 2x anamorphic magnification in the main dispersion direction.
  - A lens-doublet (identical to the collimator above) that refocuses the light.
  - A wedge of fused-silica on the exit focal plane, needed to re-position the pupil image.
  - Three flat mirrors with fold-angles adjusted to get a convenient mechanical positioning of the module.
- The main collimator, consisting of an off-axis parabola used in double pass. The diameter of the collimated beam is 400 mm in the main dispersion direction and 200 mm in the cross-dispersion direction.
- The main disperser, consisting of a R4 (76^o) echelle grating of 1600 x 200 mm.
- A wedged field lens of fused-silica, positioned at the intermediate focus. The power of the lens is used to correct the field curvature while the wedge is used to re-position the pupil image.
- A dichroic of fused-silica that reflects the "blue" light and transmits longer wavelengths. The exit face of the dichroic has a mild optical power to avoid ghosts.
- Three flat mirrors that are used to fold the light and position the arms at mechanically convenient positions.
- Two identical transfer collimators, each consisting of an on-axis parabola. An even simpler solution with a spherical mirror (as in ESPRESSO) could also be used; but the overall image quality is slightly worse.
- Two identical prisms of fused-silica each providing a 2x anamorphic magnification in the cross-disperser direction, thus re-obtaining a circular pupil (to the first order).
- Two wedges of fused-silica with a dichroic coating on the entrance face, used to split the light between the arms.
- Four cross-dispersers, consisting of transmission gratings working off-Littrow and providing an extra anamorphic magnification in the cross-dispersion direction.
- Four cameras each consisting of 2 lenses of fused-silica and 1 mirror (see Figure 10). This type of camera is the same as that developed for MOONS[6] and currently under construction. The lenses are identical in all the cameras; this simplifies the manufacturing and reduces the costs.
- A detector of 61 mm x 61 mm (size of a H4RG 4k x 4k infrared array with 15 microns pixels). The detector is behind the center of the lens (see Figure 10). This causes an obscuration at the center of the pupil with vignetting that varies along each order as shown in Figure 11.

The same design can be conveniently adapted to the other spectrometer modules obtaining the layouts shown in Figure 8 and Figure 9.
The elements listed in Table 2 are identical in all the three modules, apart for the coatings of the optical elements and the groove spacing of the echelle gratings.

Table 2 List and description of the elements common to the three spectrometer moduli.

Element	Description
Main collimator	Off-axis parabola, f=4.0 m, D-parent=1.5 m
Main disperser	Echelle R4 L=1.6 m W=0.2 m
Transfer collimators	On-axis parabola, f=2.6 m, D=0.6 m
Field lens	Fused-silica plano-convex lens, R=2.8 m, wedged 6^o
Fold mirrors	Various flats, same angles.
Anamorphic prisms	Fused-silica prisms with aperture angle 35^o
Dichroics	Fused-silica; 1 plano-convex and 2 wedged
Mechanical mounts	All the mechanical mounts from the slit image to the dichroics

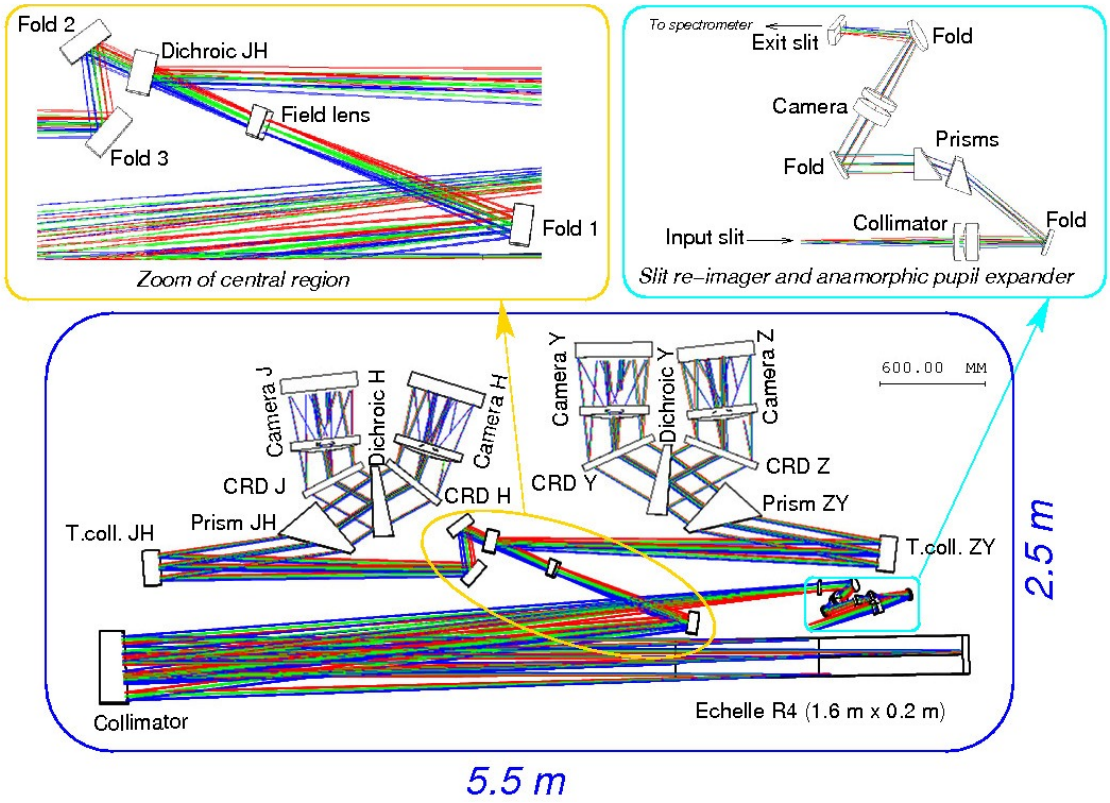

Figure 6 Layout and rays tracing of the ZYJH module

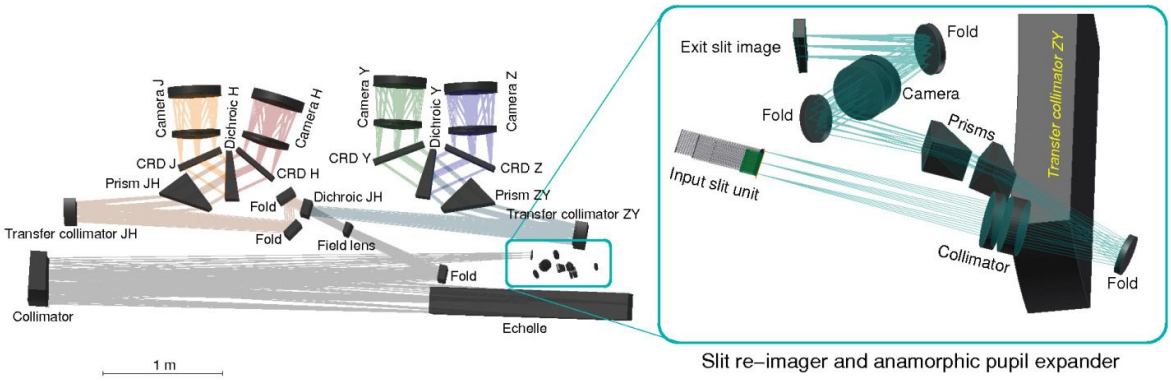

Figure 7 CAD-3D view of the ZYJH module with rays tracing

The first order parameters of the optical design are summarized in Table 3.

Table 3 First order parameters of the optics; the values are the same for all modules unless otherwise specified.

Parameter	Value
Slit length	11 arcsec (sky-projected angle); 41.6 mm at F/20
Slit width for R=100,000	0.17 arcsec (sky-projected angle); 0.64 mm at F/20
Input focal plane (before slit re-imager)	F/20, flat, telecentric, 11 x 8 arc-sec (sky-projected angle) un-vignetted field of view
Focal plane at spectrometer slit	F/10 (along dispersion) x F/20 (along cross-dispersion)
Off-axis of echelle	0.9^{o} (in the cross-dispersion direction)
Beam in main collimator	400 x 200 mm
Beam after transfer collimator	280 x 140 mm
Beam after cross disperser	280 x 290 mm
Focal aperture of cameras	F/1
Detector size	61 x 61 mm.
Detector type	ZYJH: H4RG $4k^2$ detectors with 15 microns pixels. BVRI: CCD $6k^2$ detectors with 10 microns pixels.

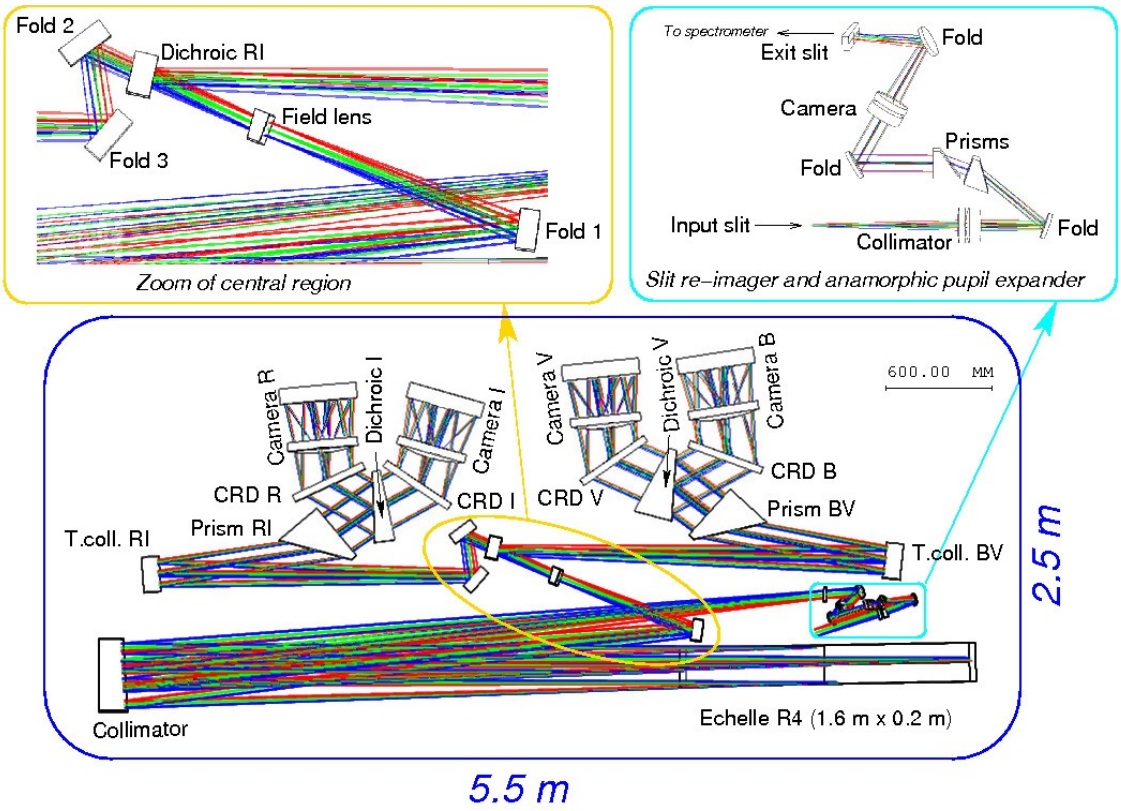

Figure 8 Layout and rays tracing of the BVRI module

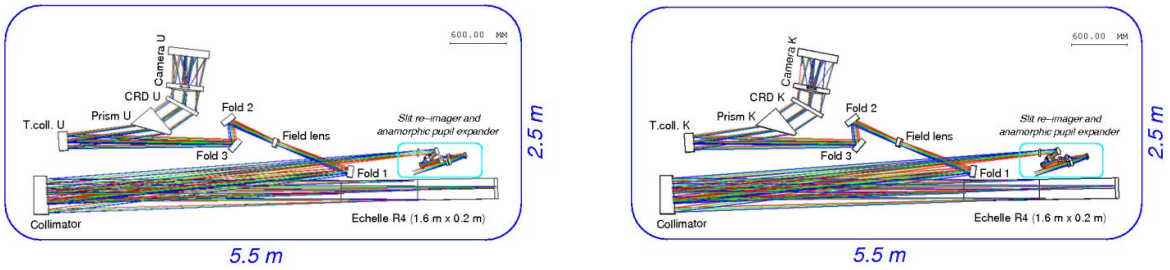

Figure 9 Layout and rays-tracing of the U module (left panel) and K module (right-hand panel).

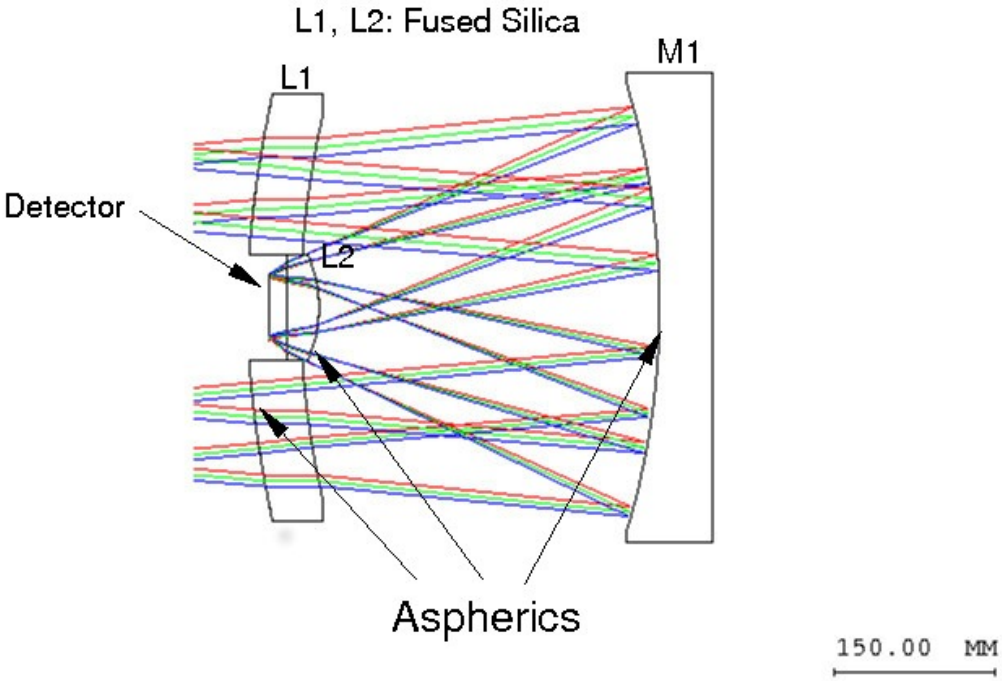

Figure 10 Detailed view of the reflective camera. L1 and L2 are identical in the 4 arms of the ZYJH and BVRI spectrometers

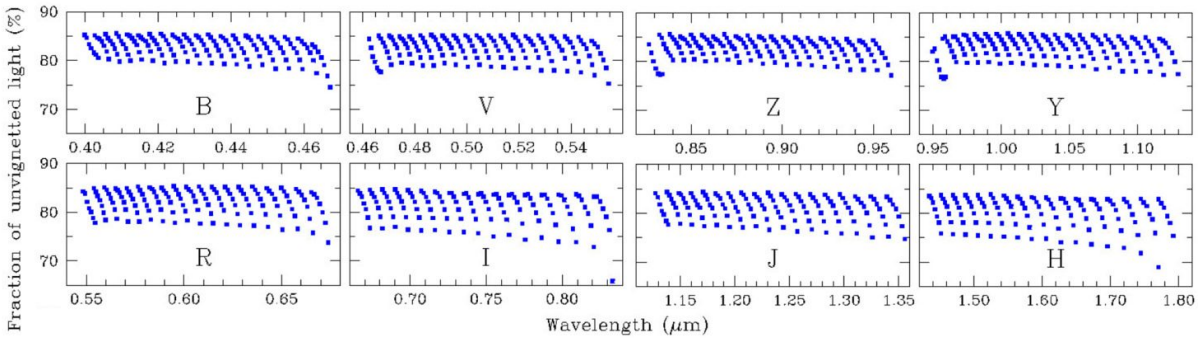

Figure 11 Effect of the central obscuration in the reflective cameras of the ZYJH and BVRI modules.

4. DISPERSERS AND SPECTRAL FORMAT

The parameters of the gratings and the spectral coverage of the modules and arms are summarized in Table 4. The corresponding spectral formats are displayed in Figure 12,
Figure 13 and Figure 14. These figures show the echellograms generated from the rays-tracing design.
The wavelength coverage of each arm is chosen to guarantee some overlap between adjacent spectral arms. The only exceptions are the J, H and K arms that are separated by regions of very poor telluric transmission (see Figure 3).
The grooves spacing of the main dispersers (echelle R4 gratings) are chosen to maximize the overall spectral coverage; i.e. with the lowest order completely filling the detector. This yields values of grooves spacing different than those available in the current catalogs and, therefore, require the production of new master gratings. Note in particular that using the standard 31.6 gr/mm would result in a BVRI module with a spectral coverage reduced to 440 - 830 nm.
The cross-dispersers are transmission gratings working in first order. Their size (340 x 380 mm), groove spacing and incidence angles are perfectly suited for the use of binary gratings lithographically etched into fused silica.

Table 4 Main parameters of the cross-disperser gratings.

Module	Echelle R4	Arm	Cross-disperser		Orders	Wavelength coverage (nm)
			gr/m	AOI		
ZYJH	16.00 gr/mm	H	465	22.9°	68 - 84	1435 - 1800
		J	730	32.9°	90 - 107	1128 - 1356
		Y	930	35.4°	108 - 127	950 - 1128
		Z	1240	41.1°	127 - 146	827 - 955
BVRI	34.50 gr/mm	I	1000	22.3°	68 - 84	666 - 833
		R	1410	33.3°	84 - 102	549 - 674
		V	1860	32.6°	102 - 121	483 - 555
		B	2490	39.4°	121 - 140	400 - 467
U	67.00 gr/mm	U	2240	27.2°	72 - 87	330 - 405
K	11.95 gr/mm	K	360	27.8°	72 - 86	1877 - 2405

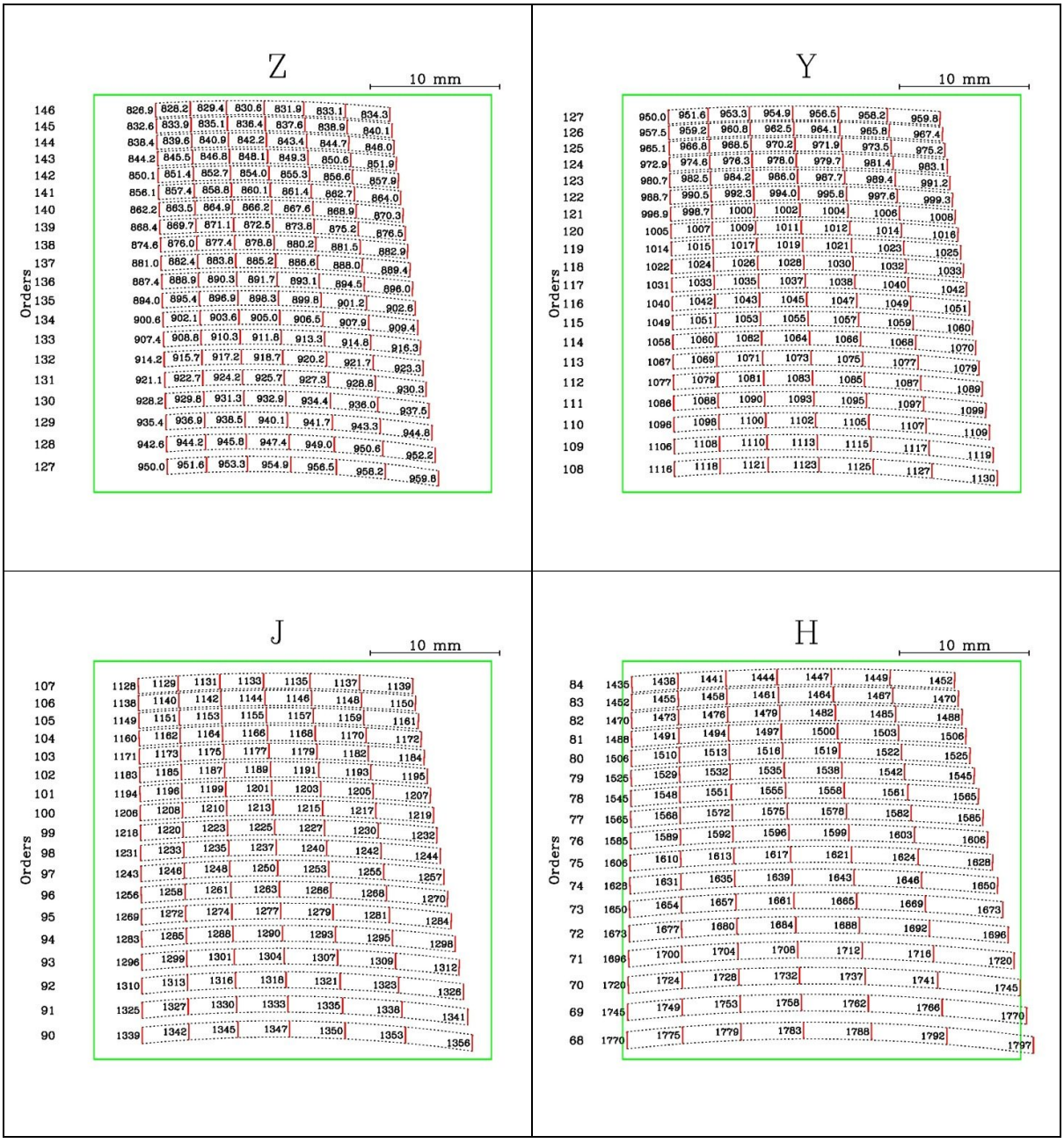

Figure 12 Echellograms and spectral format of the 4 arms of the ZYJH module; generated from the rays tracing. The green square represents the area of the 61x61 mm detector. Wavelengths are in nm.

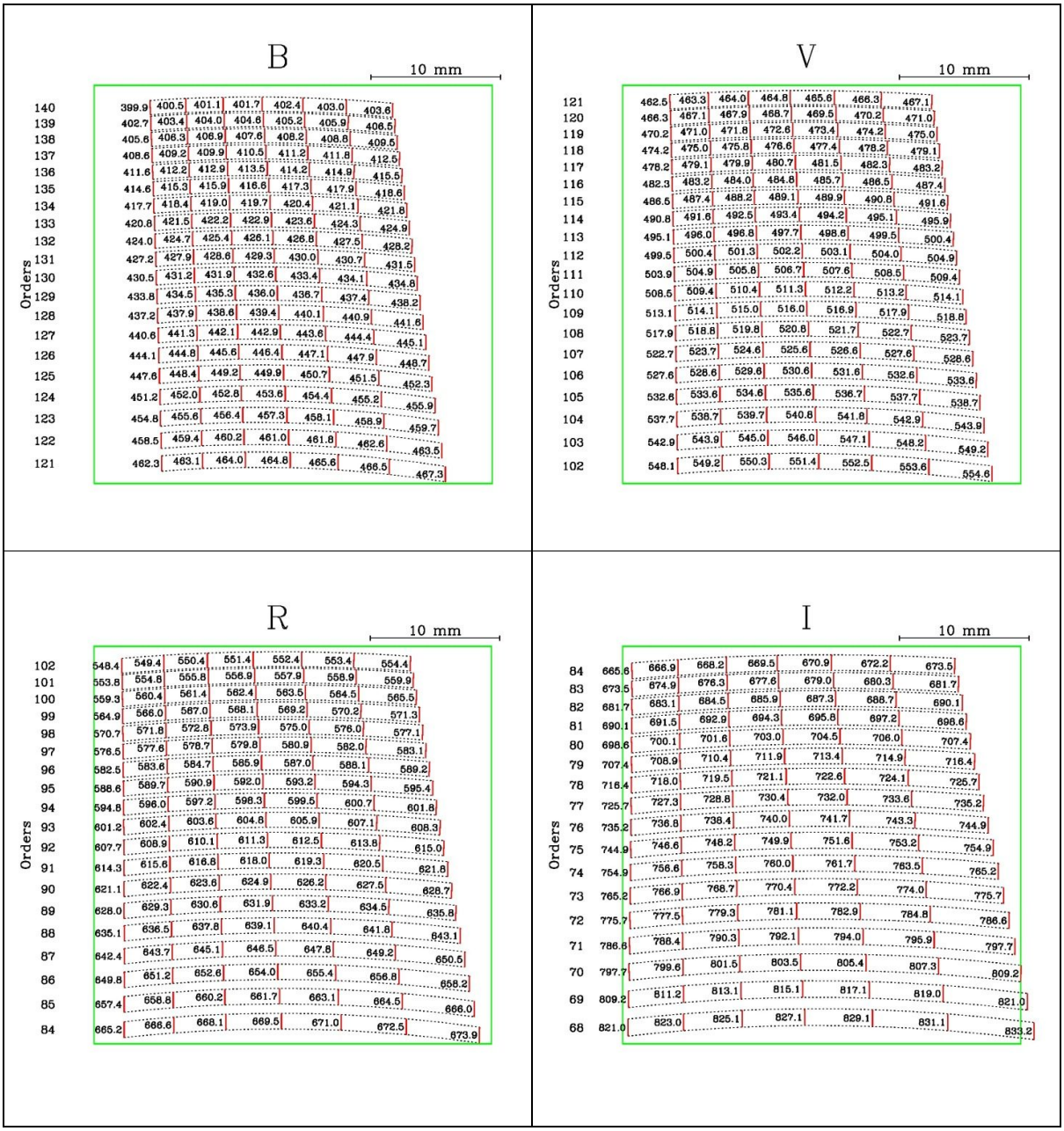

Figure 13 Echellograms and spectral format of the 4 arms of the BVRI module; generated from the rays tracing. The green square represents the area of the 61x61 mm detector. Wavelengths are in nm.

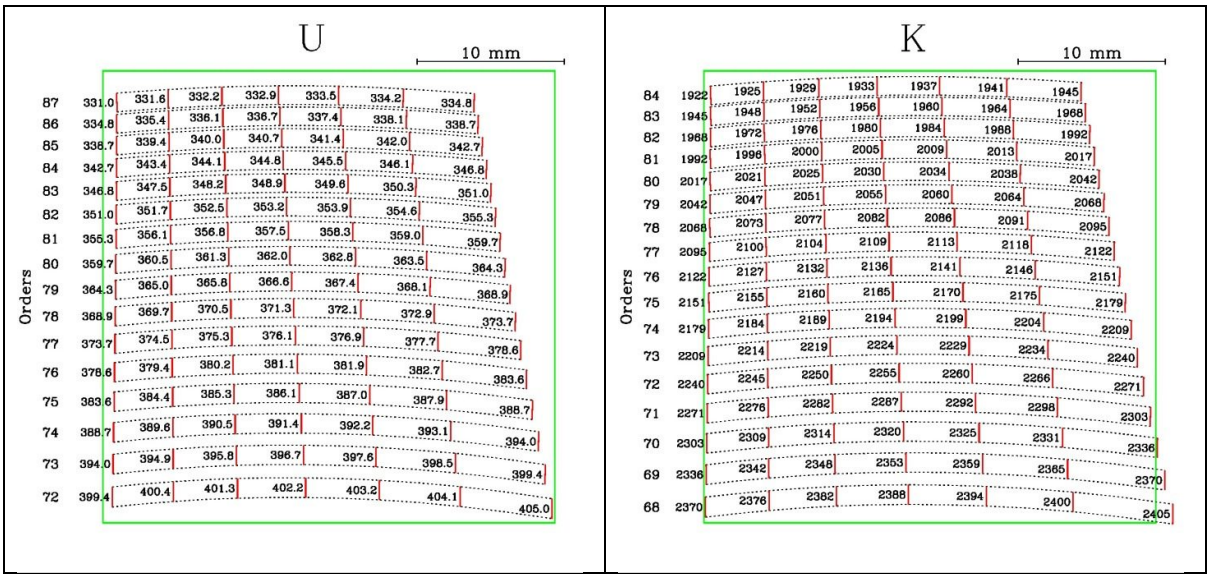

Figure 14 Echellograms and spectral format of the U and K modules; generated from the rays tracing. The green square represents the area of the 61x61 mm detector. Wavelengths are in nm.

5. IMAGE QUALITY

The optical quality of the entire spectrometer can be conveniently evaluated in terms of the diameters with ensquared energies equal to 50%, 80% and 95%. These parameters are computed at different wavelengths, orders and spatial positions along the slit; thus covering the whole echellograms. The diameters of ensquared energies can be expressed in microns and in terms of the ratio between the diameter of encircled energies and the geometrical width of the slit image onto the detector at a given wavelength, order and position along the slit. The latter ratio provides direct information of the fraction of light falling inside the slit image. The results are displayed in Figure 15, Figure 16 and Figure 17. The values are remarkably good; for BVRI the optical quality is similar to that achieved in the optical design of ESPRESSO (see the comparison in Figure 18).

The image quality at the extreme wavelengths (K and U modules) is slightly deteriorated by the chromatic aberration introduced by the fused silica lenses in the cameras. Although better results could be in principle obtained using CaF_2 elements; however this solution is risky - because it requires CaF_2 crystals of size larger than those currently produced - and it would make the system much more expensive and difficult to handle.

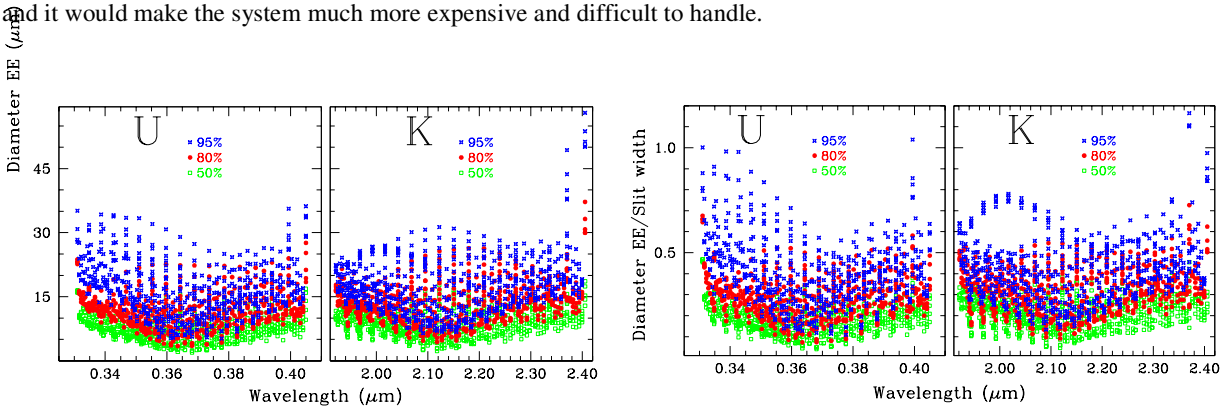

Figure 15 Diameter of encircled energies over the echellograms of the U and K spectrometers.

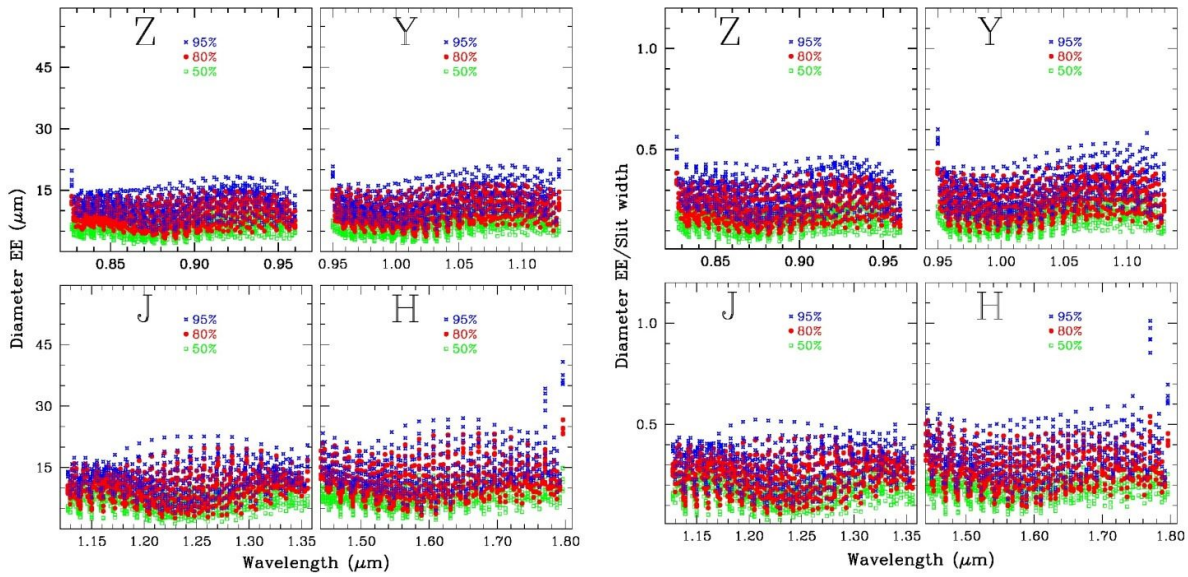

Figure 16 Diameter of encircled energies over the echellograms of the ZYJH spectrometer.

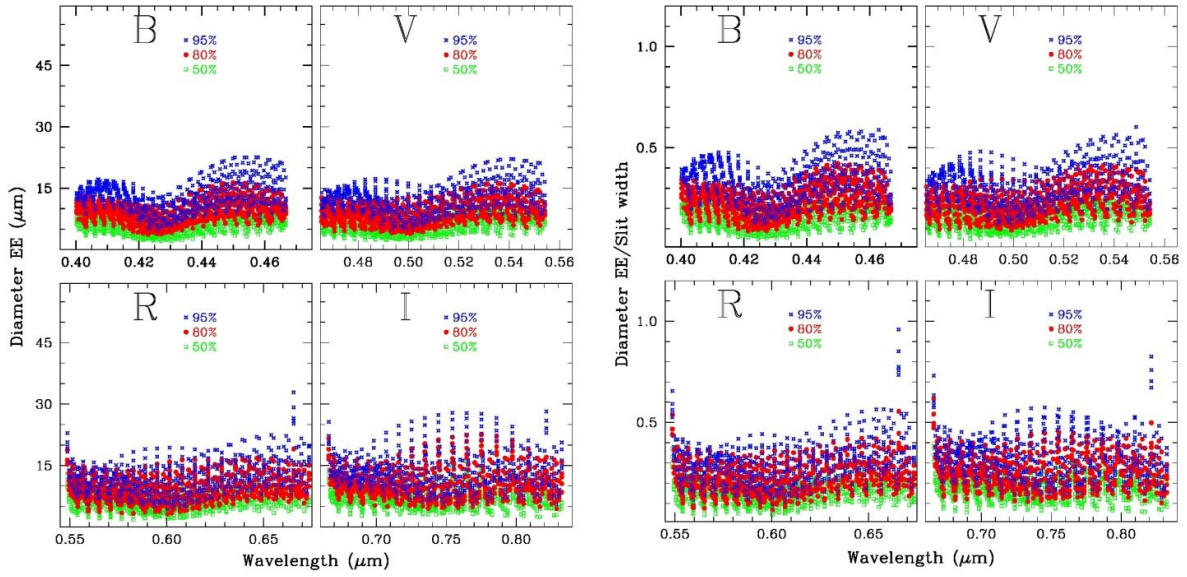

Figure 17 Diameter of encircled energies over the echellograms of the BVRI spectrometer.

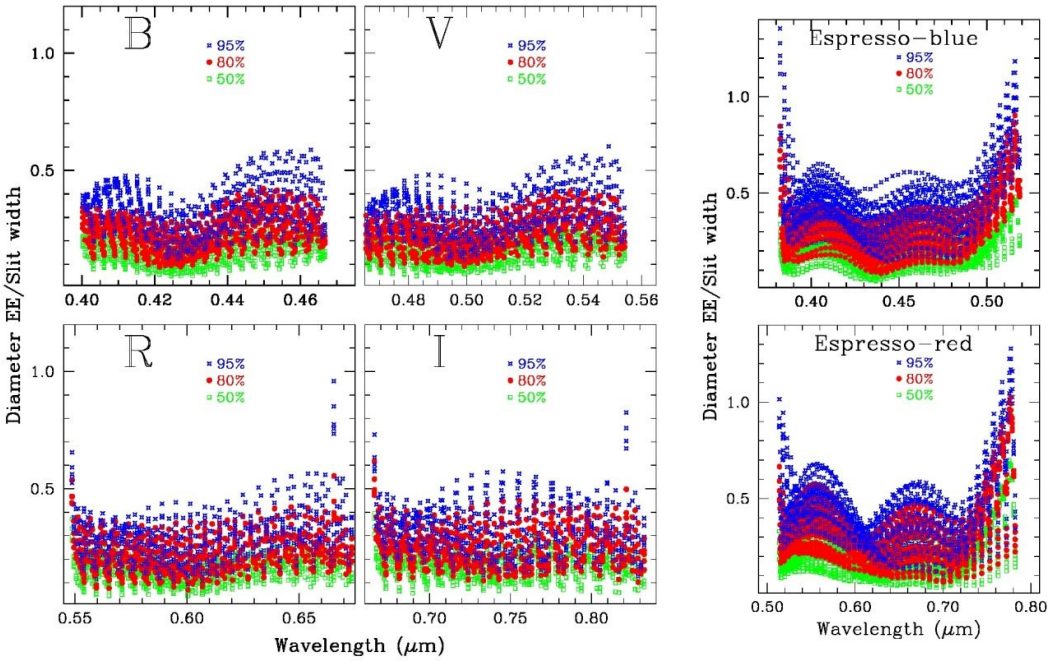

Figure 18 Comparison between the image qualities of the BVRI module (left) and ESPRESSO (right). In both plots the diameters of the encircled energies are computed over the whole echellogram and are normalized to the geometrical width of the slit image, thus providing a direct comparison independent on the scale of the image on the detector.

6. ALTERNATIVE DESIGN WITH LENS-CAMERAS

An alternative design for the BVRI module with refractive cameras (i.e. cameras with only lenses) is shown in Figure 19. It uses larger detectors (92 mm x 92 mm) and slower beams at the focal plane (F/1.6). The lens-cameras are much larger (about 1 x 0.5 m) and heavier (about 200 kg) than the reflective cameras (see Figure 20). The lenses are made by fused silica, F2 and BK7 (or equivalent); i.e. the most popular and better controlled glasses that are normally available in large enough sizes and that have low internal absorption over the whole 400-1000 nm range. A minimum of six lenses with three aspheric surfaces are needed to obtain good images. The final optical quality is slightly worse than that achieved with reflective cameras (see Figure 21). The total thickness of glass is such that the overall throughput and image quality may be deteriorated by the internal absorption and non-homogeneities of the glasses. Moreover, the manufacturing and alignment errors of the many surfaces may introduce other aberrations. In practice, the efficiency that one formally gains avoiding the central obscuration could be partially lost by the practical problems related to such complex lens-cameras. Cost is another important drawback of lens-cameras.

Solutions with lenses are much more difficult (or even impossible) to achieve for the infrared modules because of the very fast focal ratio (F/1) imposed by the size of the IR detector and because of the very limited choice of glasses that are sufficiently transparent in the required spectral range and available in large size/thickness (in practice only fused-silica and CaF_2). More details can be found in the trade-off analysis for the MOONS optics[6].

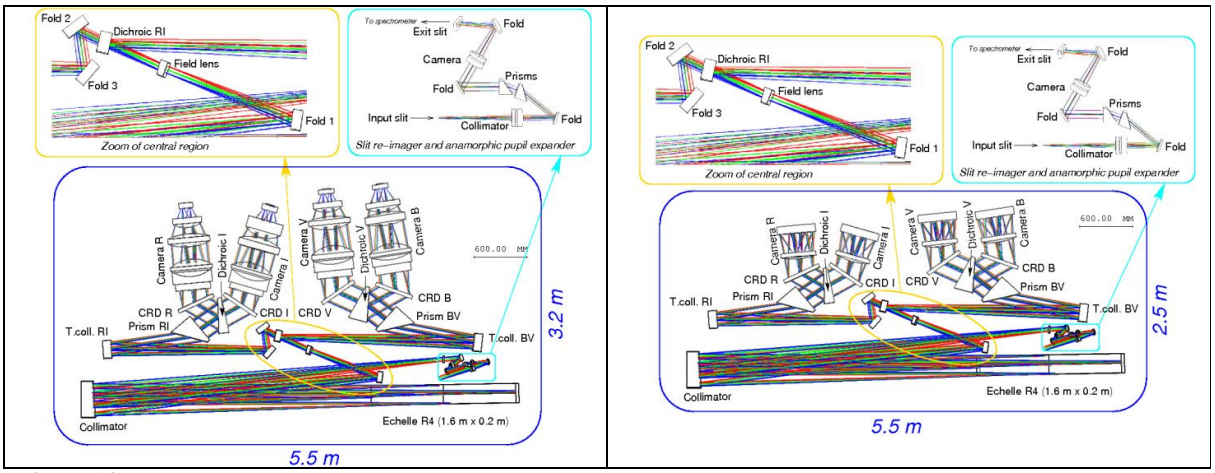

Figure 19 Comparison between the layouts of BVRI module with lens-cameras (leftl) and with reflective cameras (right-hand panel). Apart for the cameras, all the other elements are identical.

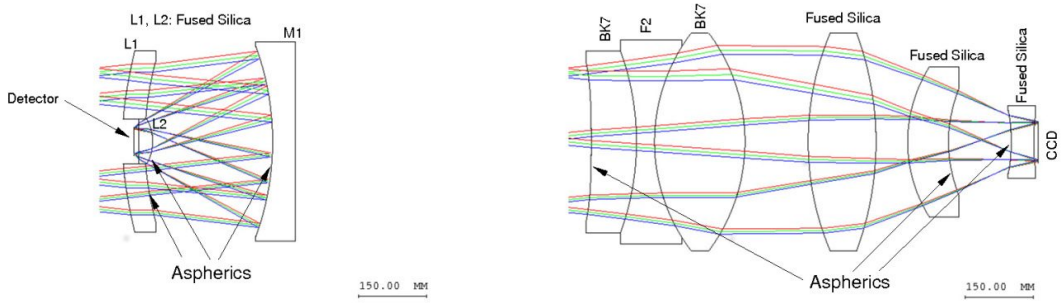

Figure 20 Layouts and rays-tracings of a reflective (left) and a lens camera. The detector in the lens camera is tilted.

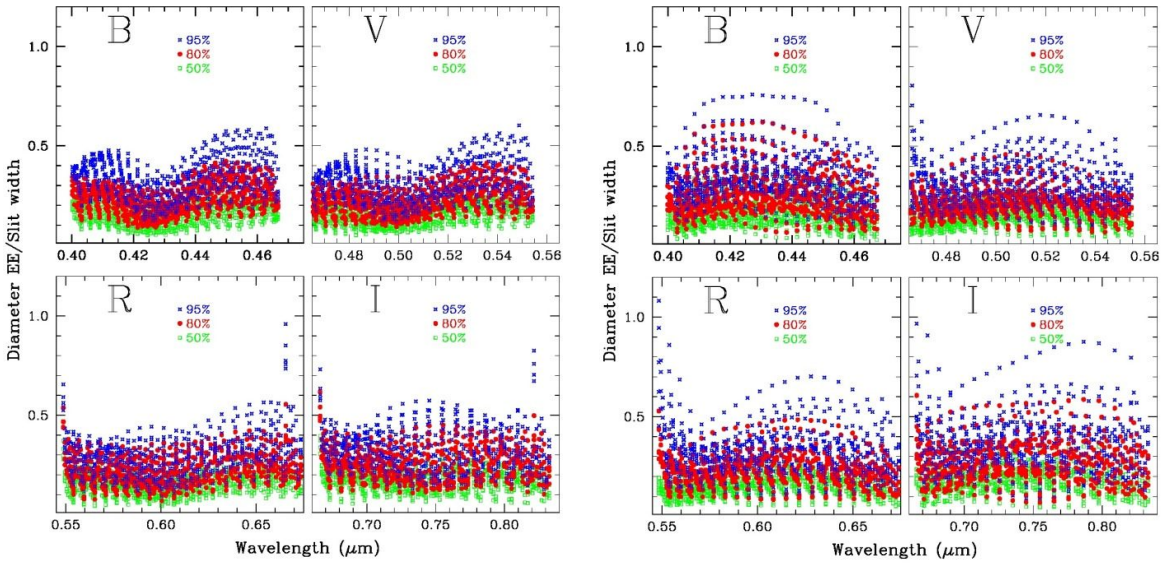

Figure 21 Comparison between the image qualities of the BVRI module with reflective cameras (left) and with lens cameras (right-hand panel). In both plots the diameters of the encircled energies are computed over the complete echellograms and are normalized to the geometrical width of the slit image, thus providing a direct comparison independent on the scale of the image on the detector.

7. INPUT SLIT

The entrance of each spectrometer module consists of an optical system that re-images the input focal plane onto the virtual slit of the spectrometer (see Figure 6, Figure 7 and Figure 8). The re-imaging optics have an unvignetted field of view of 11 x 8 arcsec (sky projected angles). Therefore, they can be used to re-image the light from many parallel slits that can be separately illuminated through dedicated fiber bundles. Each fiber bundle corresponds to an observing mode and terminates in a linear array of micro-lenses, as shown in Figure 22.

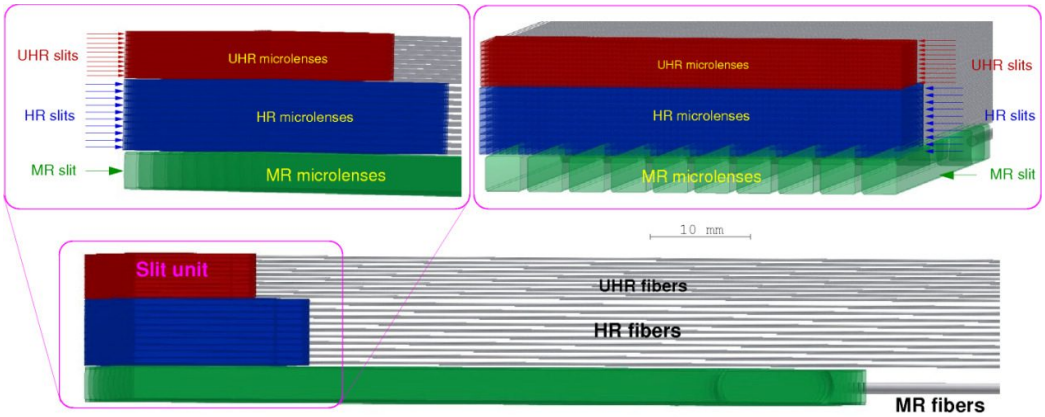

Figure 22 CAD views of the arrays of micro-lenses and fibers at the input focal plane of a spectrometer module.

Each micro-lens consists of a lens doublet that produces a sharp, quasi-telecentric and chromatically corrected image of the pupil at F/20.

Figure 23 shows the layout and rays-tracing of the micro-lenses for the HR, UHR and MR modes of the ZYJH module. They are designed assuming that the intrinsic focal aperture of the fiber is F/3.5. The micro-lenses in the spectrometer have a rectangular shape. The same micro-lenses can be used in the front-end to receive the light from the telescope, and in the fiber-to-fiber interface to double-scramble the light of a whole fiber-bundle. The only differences are their external shape - that must be hexagonal - and organization on a quasi-circular field of view. Therefore, the large number of identical micro-lenses and fiber interfaces, that are needed to implement all the observing modes, can be most conveniently manufactured via an industrial process specifically set-up for this project.

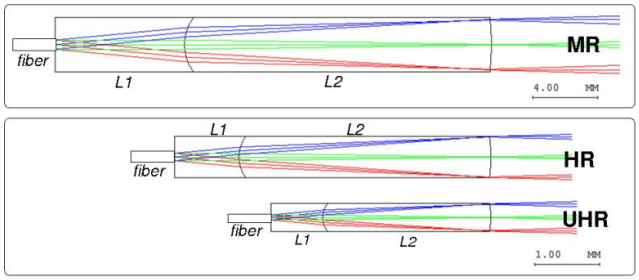

Name	L1 (t,R in mm)	L2 (t,R in mm)	F# fiber	F# lens	Ø core (mm)	D lens (mm)	Maximum light losses for all fields and wavelengths
HR	SBSL7 t=1.00 R1 flat R2=0.510 K2=-4.0	SLAM55 t=4.00 R1=0.510 K1=-4.0 R2=2.407	F/3.5	F/20	0.113	0.646	4%
UHR	SBSL7 t=0.80 R1 flat R2=0.350 K2=-4.0	SLAM55 t=2.60 R1=0.350 K1=-4.0 R2=1.71	F/3.5	F/20	0.075	0.430	5%
MR	SBSL7 t=8.0 R1 flat R2=2.80 K2=-3.0	SLAM55 t=19.0 R1=2.80 K2=-3.0 R2=15.1	F/3.5	F/20	0.570	3.40	2%

Main parameters of micro-lenses (glued doublets) for the HIRES ZYJH spectrometer module.
L1, L2: t=thickness, R=radius of curvature, K=conic constant. Fiber is glued to first (flat) surface of L1.
F# fiber : nominal aperture of light beam at the fiber; beams are telecentric .
F# lens: nominal aperture of light beam at the micro-lens; beams are telecentric.
Ø core: diameter of fiber core.
D lens: size of the lens.
Includes light losses produced by blurring of images, by deviations from telecentricity, and by variations of the beam apertures. Maximum values among all fields and wavelengths; average values are smaller.

Figure 23 Layout, rays-tracing and main parameters of the micro-lenses.

8. COMPARISON WITH THE DESIGN OF OTHER HIGH RESOLUTION SPECTROMETERS

To evaluate the overall capabilities of a given spectrometer it is convenient to combine its parameters into a single figure of merit or "Spectrometer Equivalent Power" (S.E.P.). This quantity is proportional to the spectral resolving power (*R*), to the sky-projected area of the entrance aperture and to the number of spectral resolution elements that are simultaneously covered in the spectrum. Numerically:

$$\text{S.E.P.} = \left(\frac{R}{10^5}\right)\left(\frac{\Omega_{aperture}}{1\ \text{sq.arcsec}}\right)\left(\log_2\frac{\lambda_{max}}{\lambda_{min}}\right)\left(\frac{\eta_{\lambda\text{-}coverage}}{100\%}\right)$$

A high resolution spectrometer with S.E.P. greater than unity can effectively operate under normal seeing conditions and acquire high resolution spectra covering a wide wavelengths range (one octave). Instead, instruments with S.E.P. much lower than unity require some improvement of the telescope PSF (i.e. AO correction) and/or must work over a reduced wavelengths range. For a given spectrometer, the value of the sky-projected aperture is proportional to $(1/D_{Telescope})^2$. Consequently, modern spectrographs that are effectively operating on 4m class with S.E.P.~10 (e.g. HARPS, CARMENES) would have values of S.E.P.<0.1 if mounted on the ELT. Even replicating the most powerful spectrograph built so far – i.e. ESPRESSO – one would still fall short by a factor of two.

The above considerations are summarized in Table 5 that includes a few representative optical/IR HR spectrographs that are operating on, or are under construction for existing telescopes. The table also includes the designs of seeing-limited HR spectrometers for ELT's, namely G-CLEF (GMT), MTHR (TMT), CODEX (first phase-A of ELT) and HIRES (this project). The entries "ESPRESSO*BVRI" and "CODEX*BVRI" are spectrographs similar to ESPRESSO and CODEX with parameters re-adjusted to get $R=10^5$ and shift the maximum wavelength to 830 nm.

Table 5 Parametric comparison of some high resolution spectrographs.

Spectrometer name	Parameters on ELT					
	Resolving power	Sky-projected aperture (sq.arcsec)	Minimum wavelength (nm)	Maximum wavelength (nm)	Spectral coverage	S.E.P.
GIANO	50,000	0.03	950	2400	85%	0.01
NIRPS	100,000	0.02	980	1800	100%	0.02
HARPS	120,000	0.09	380	690	100%	0.09
CARMENES	100,000	0.10	520	960	100%	0.09
ESPRESSO	130,000	0.51	380	780	100%	0.69
ESPRESSO*BVRI	100,000	0.66	400	830	100%	0.69
G-CLEF[7] (GMT)	130,000	0.37	350	950	100%	0.69
CODEX	130,000	1.6	370	720	100%	2.0
CODEX*BVRI	100,000	1.9	400	830	100%	2.0
HIRES-BVRI	100,000	1.9	400	830	100%	2.0
HIRES-ZYJH	100,000	1.9	830	1800	95%	2.0
MTHR[8] (TMT)	100,000	4.8	310	1000	100%	8.1

To better understand the intrinsic characteristics and limits of seeing-limited HR spectrometer it is convenient to compare in some details the designs of ESPRESSO and of the instruments so far developed for ELTs.

Figure 24 shows a comparison between G-CLEF and ESPRESSO. The two spectrographs have the same value of S.E.P. and are remarkably similar. They both have a grating-echelle 1.2 meters long; and two cross disperser arms with F/2.5 cameras each feeding a detector of 92x92 mm^2. The main differences are the length of the slit (longer in ESPRESSO) and the wavelength coverage (broader in G-CLEF). The two quantities compensate each-others, i.e. the design of G-CLEF gives higher priority to the wavelength coverage; and it accepts a smaller entrance aperture.

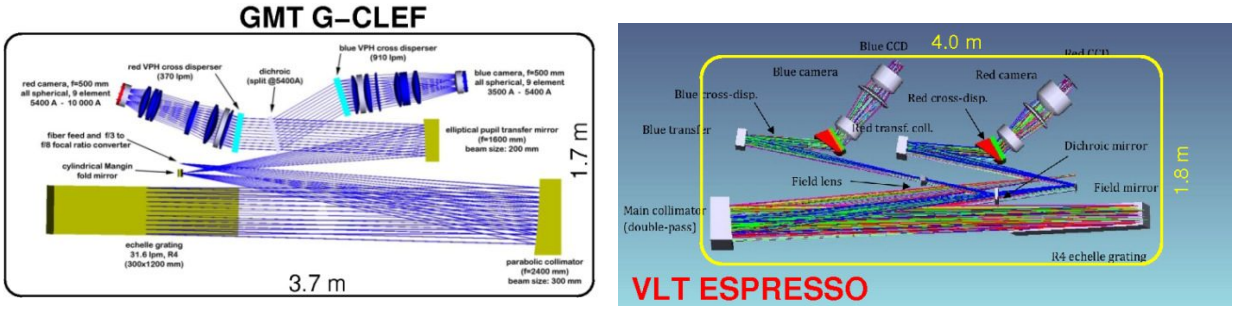

Figure 24 Layouts of the G-CLEF (left panel) and ESPRESSO spectrometers

Figure 25 shows a comparison between ESPRESSO and CODEX, the instrument proposed during the first phase-A of the ELT. The S.E.P. of CODEX is a factor of 2.9 larger because it has a longer echelle grating (1.6 m) and a much longer slit that requires 4 cross disperser arms. Another important difference is the main collimator: CODEX uses three aspheric mirrors, while ESPRESSO uses a single parabolic mirror. For this reason the collimator of CODEX is more compact.

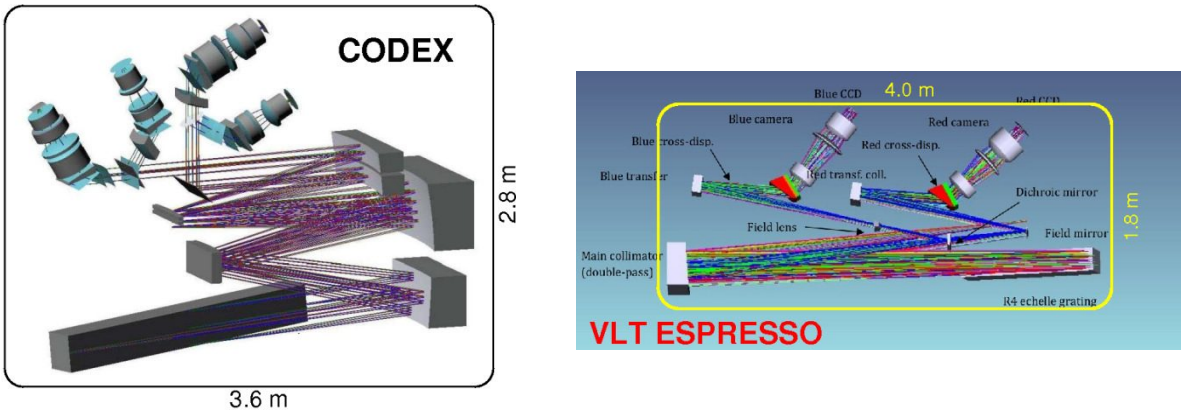

Figure 25 Layouts of the CODEX (left panel) and ESPRESSO spectrometers

Figure 26 shows a comparison between ESPRESSO and HIRES. The latter has a larger S.E.P. because it has a longer echelle grating (1.6 m) and a longer slit that requires 4 cross disperser arms. Apart for the above differences, the overall layout of HIRES is similar to ESPRESSO; indeed HIRES could be called a "DOUBLE-ESPRESSO".

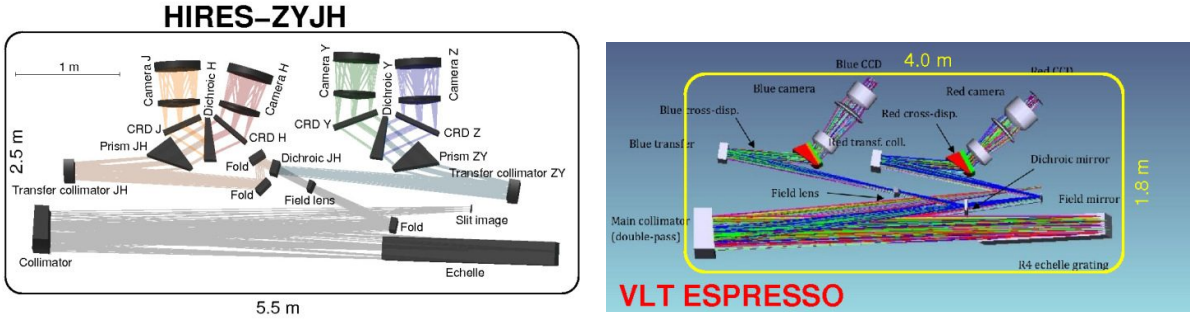

Figure 26 Layouts of the HIRES (left panel) and ESPRESSO spectrometers

Figure 27 shows a comparison between the layouts of HIRES and MTHR, the concept design for the HR spectrograph of the TMT. MTHR achieves a much larger value of S.E.P. because it employs two echelle-gratings of 3.5 m. Its overall design is similar to a classical echelle spectrograph: clean, simple but very large.

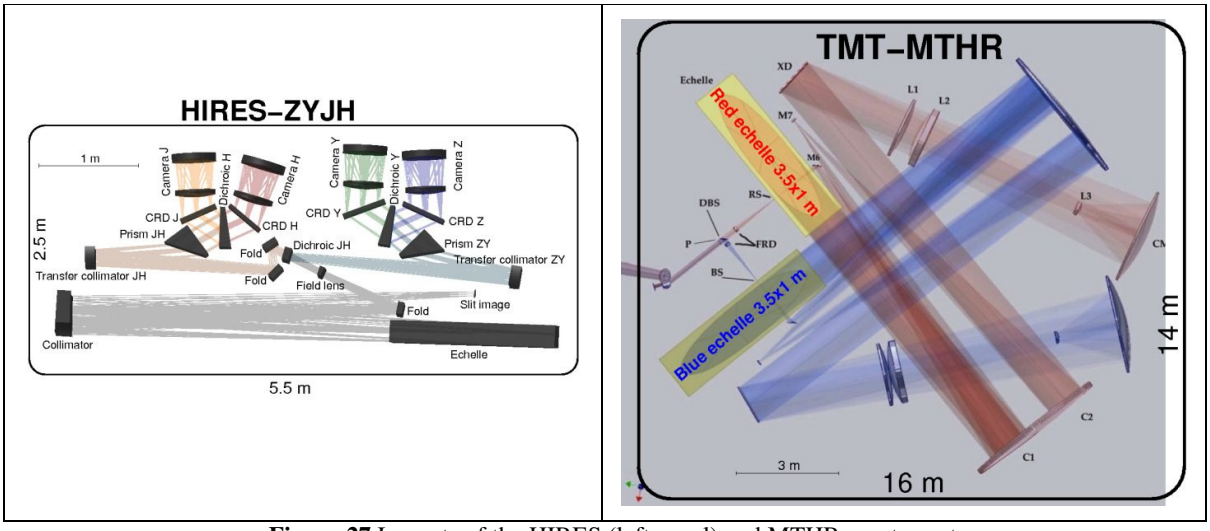

Figure 27 Layouts of the HIRES (left panel) and MTHR spectrometers

9. GENERAL SCALING LAWS FOR SPECTROMETER DESIGN

The quantities that drive the size and the cost of a spectrometer are intrinsically related to the fundamental principle of throughput conservation (A*Omega = constant). The key parameters are as follows

i. The length of the main-dispersion grating (echelle) that determines the product between the spectral resolving power (R) and the sky-projected width (*theta-slit*) of the slit. Numerically:

$$R = 1.03 \cdot 10^4 \left(\frac{\theta_{slit}}{1''}\right)^{-1} \left(\frac{L_{grating}}{1.0\ \mathrm{m}}\right) \left(\frac{\sin\ \theta_{grating}}{\sin 76^\circ}\right) \left(\frac{D_{tel}}{39\ \mathrm{m}}\right)^{-1}$$

ii. The total detector-area needed to collect the complete spectrum (F_{camera} is the aperture focal ratio of each camera)

$$A_{total} = 60\ \mathrm{cm}^2 \left(\frac{R}{10^5}\right) \left(\frac{\Omega_{aperture}}{1\ \mathrm{sq.\,arcsec}}\right)^2 \left(\log_2 \frac{\lambda_{max}}{\lambda_{min}}\right) \left(\frac{\eta_{\lambda\text{-}coverage}}{100\%}\right) \left(\frac{F_{camera}}{1}\right)^2 \left(\frac{D_{tel}}{39\ \mathrm{m}}\right)^2$$

$$A_{total} = 60\ \mathrm{cm}^2\ \ (\mathrm{S.E.P.}) \left(\frac{F_{camera}}{1}\right)^2 \left(\frac{D_{tel}}{39\ \mathrm{m}}\right)^2$$

iii. The number of separated arms/channels that are needed to cover the complete spectrum. This parameter is determined by the practical limits on the size of the beam at the cross-disperser gratings (D_{CRD}) and on the maximum range of angles that can be accepted by a camera. Moreover, the number of CRD-arms that can be coupled to a single echelle grating is limited by the need of creating a separate image of the pupil on each CRD grating. These constraints yield

$$N_{\text{CRD arms}} \simeq 2 \cdot N_{slits} \cdot (\text{S.E.P.}) \left(\frac{D_{\text{beam at CRD}}}{0.3\ \text{m}} \right)^{-1} \left(\frac{D_{tel}}{39\ \text{m}} \right)^{2}$$

$$N_{\text{CRD arms}} \leq 4 \cdot N_{\text{echelle gratings}}$$

In the above equation N_{slits} is the number of separated slit images created after the main collimator. This parameter was introduced in the design of CODEX as an alternative solution to split in wavelengths the CRD channels. The conceptual difference is schematized in Figure 28.
The net result is that a given spectral coverage and aperture on sky can only be achieved using the same echelle grating, the same number of CRD arms and the same A*Omega for each camera.

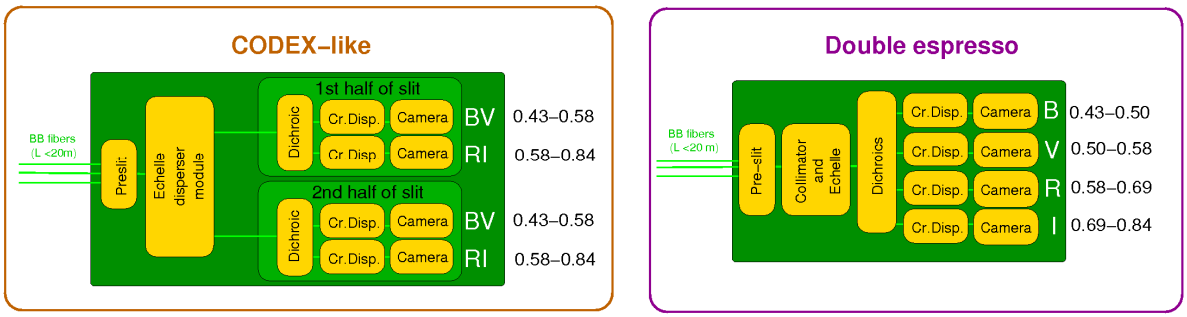

Figure 28 Schematic comparison between slit-spitting and wavelength-splitting solutions in HR spectrometers

10. ACKNOWLEDGEMENTS

This work was financially supported by the Italian Institute of Astrophysics through the grant and "T-REX: Italian Technologies for ELT"

REFERENCES

[1] Pasquini, L.; Cristiani, S.; Garcia Lopez, R.; et al.; "*CODEX"*, SPIE, 7735E-2FP (2010)
[2] Origlia, L.; Oliva, E.; Maiolino, R.; et al..; "*SIMPLE: a high-resolution near-infrared spectrometer for the E-ELT*", SPIE, 7735E-2BO (2010)
[3] Marconi, A.; Di Marcantonio, P.; Maiolino, R.; et al.; "*ELT-HIRES, the high resolution spectrograph for the ELT: results from the Phase A study*", SPIE, 10702-70 (2018); this conference
[4] Cabral, A.; Aliverti, M; Coehlo, J.; et al.; "*ELT-HIRES the high resolution spectrograph for the ELT: the design of the front end*", SPIE, 10702-358 (2018); this conference
[5] Tozzi, A.; Oliva, E.; Sanna, N.; et al.; "*ELT-HIRES, the high resolution spectrograph for the ELT: the IFU-SCAO module*", SPIE, 10702-319 (2018); this conference
[6] Oliva, E.; Delabre, B.;Tozzi, A.; et al.; "*Toward the final optical design of MOONS, the Multi-Object Optical and Near-Infrared spectrograph for the VLT*", SPIE, 9908-7RO (2016)
[7] Fürész, G.; Epps, H.; Barnes, S.; et al.; "*The G-CLEF spectrograph optical design*", SPIE 9147-9GF (2014)
[8] Vogt, S.; Rockosi, C.; Cowley, D.; *"The MTHR Spectrometer"*, TMT.INS.PRE.07.012.REL01 (2007)